Detecting synchronization of self-sustained oscillators by external driving with varying frequency

Alexander E. Hramov* and Alexey A. Koronovskii†

Faculty of Nonlinear Processes, Saratov State University, Astrakhanskaya, 83, Saratov, 410012, Russia

Vladimir I. Ponomarenko‡ and Mikhail D. Prokhorov

Saratov Department of the Institute of RadioEngineering and Electronics of Russian Academy of Sciences, Zelyonaya, 38, Saratov, 410019, Russia

(Received 1 June 2005; published 13 February 2006)

We propose a method for detecting the presence of a synchronization of a self-sustained oscillator by external driving with linearly varying frequency. The method is based on a continuous wavelet transform of the signals of the self-sustained oscillator and external force and allows one to distinguish the case of true synchronization from the case of spurious synchronization caused by linear mixing of the signals. We apply the method to a driven van der Pol oscillator and to experimental data of human heart rate variability and respiration.

PACS number(s): 05.45.Xt, 05.45.Tp

I. INTRODUCTION

It is well known that interaction between nonlinear oscillatory systems including the ones demonstrating chaotic behavior can result in their synchronization. Various types of synchronization between oscillatory processes have been intensively studied in many physical, chemical, and biological systems [1–6]. Of particular interest in recent years is the investigation of synchronization in living organisms whose activity is determined by interaction of a great number of complex rhythmic processes. The underlying sources of these oscillatory processes often cannot be measured separately, but only superpositions of their signals are accessible. For example, in electroencephalography recordings on the scalp the measured signals are the superpositions of the signals generated by various interacting sources. As a result, one can detect spurious synchronization between brain sources and come to wrong biological conclusions [7]. This situation is typical for many multichannel measuring devices. One faces a similar problem studying synchronization between the rhythms of the cardiovascular system (CVS). The most significant oscillating processes governing the cardiovascular dynamics, namely, the main heart rhythm, respiration, and the process of blood pressure slow regulation with the fundamental frequency close to 0.1 Hz, appear in various signals: electrocardiogram (ECG), blood pressure, blood flow, and heart rate variability (HRV) [8]. This fact impedes studying their synchronization.

Synchronization between the main rhythmic processes in the human CVS has been reported in Refs. [5,9–12]. It has been found that the systems generating the main heart rhythm and the rhythm of slow regulation of blood pressure can be treated as self-sustained oscillators and the respiration can be regarded as an external forcing of these systems [11,12]. However, at respiration frequencies close to 0.1 Hz it becomes difficult to distinguish the case of true synchronization between the respiration and the process of blood pressure regulation from the case of spurious synchronization caused by the presence of the respiratory component in the HRV and blood pressure signals used for the analysis of the rhythm with the basic frequency of about 0.1 Hz. Actually, the presence of external forcing can result in linear mixing of the driving signal and the signal of the self-sustained oscillator without any synchronization. Another possible case is the simultaneous presence of mixing of the signals and their synchronization.

In this paper we propose a method for detecting synchronization of a self-sustained oscillator by external driving with linearly varying frequency. The method is based on a wavelet transform of both the external signal and the self-sustained oscillator signal and allows one to distinguish true synchronization from the spurious one caused by linear mixing of the signals. The principal interest of our approach is that we vary the frequency of external signal. We verify our method by applying it to a driven van der Pol oscillator and to experimental data of human HRV and respiration. It should be noted that synchronization between the different rhythmic processes can be detected also from the analysis of univariate data [10,13–17]. However, in the present paper we use only bivariate signals for detecting synchronization.

The paper is organized as follows. In Sec. II the models for studying the effects of synchronization and mixing are considered. In Sec. III we describe the method for detecting synchronization using the continuous wavelet transform. Section IV presents the results of the method application to a driven asymmetric van der Pol oscillator. In Sec. V the synchronization between the respiration and the process of slow regulation of blood pressure is studied. In Sec. VI we summarize our results.

---

*Electronic address: aeh@cas.ssu.runnet.ru

†Electronic address: alkor@cas.ssu.runnet.ru

‡Electronic address: vip@sgu.ru

II. MODELS

The universality of the phenomena observed in periodically driven self-sustained oscillators of physical and physiological nature has been discussed in Refs. [5,10]. It has been shown there that qualitatively the same features of synchronization are observed in the case of periodic driving of a van der Pol oscillator and in the case of respiratory forcing of the heartbeat and the process with the basic frequency of about 0.1 Hz. Let us consider the asymmetric van der Pol oscillator under external forcing with linearly increasing frequency as a model for studying interaction between the respiration and the process of blood pressure slow regulation.

The periodically driven asymmetric van der Pol oscillator is described by the following equation:

$$\ddot{x} - \mu(1 - \alpha x - x^2)\dot{x} + \Omega^2 x = K \sin \varphi(t), \qquad (1)$$

where $\mu=1$ is the parameter of nonlinearity, $\Omega=0.24\pi$ is the natural frequency, and K and $\varphi(t)$ are, respectively, the amplitude and phase of the external force. The phase

$$\varphi(t) = 2\pi[(a + bt/T)]t \qquad (2)$$

defines the linear dependence of the driving frequency $\omega_d(t)$ on time:

$$\omega_d(t) = \frac{d\varphi(t)}{dt} = 2\pi(a + 2bt/T), \qquad (3)$$

where $a=0.03$, $b=0.17$, and $T=1800$ is the maximal time of computation. We choose these parameter values to compare the results of simulation with those obtained in investigation of experimental signals of respiration and HRV (see Sec. V).

The case $\alpha=0$ in Eq. (1) corresponds to the classical van der Pol oscillator with symmetric limit cycle. As a result of phase portrait symmetry, the power spectrum of oscillations has only odd harmonics $(2n+1)f_0$, $n=1,2,\ldots$, of the basic frequency f_0. Since the second harmonic $2f_0$ of the process with the basic frequency close to 0.1 Hz is well pronounced in the power spectrum, we consider the modified van der Pol oscillator (1) with $\alpha=1$.

The difference between the frequency ω_0 of self-sustained oscillations and the natural frequency Ω is due to the effect of nonlinearity [$f_0=\omega_0/2\pi=0.106$ in Fig. 1(a)]. In the case of an asymmetric van der Pol oscillator this difference is greater [$f_0=0.098$ in Fig. 1(b)].

To compare the case of synchronization of oscillations by external driving with the case of mixing of the signals we consider the superposition of the signals

$$x_\Sigma(t) = x(t) + R \sin \varphi(t), \qquad (4)$$

where $x(t)$ is the signal of the autonomous asymmetric van der Pol oscillator and $R \sin \varphi(t)$ is the additive signal with amplitude R, phase $\varphi(t)$, and varying frequency (3).

III. METHOD OF DETECTING SYNCHRONIZATION USING CONTINUOUS WAVELET TRANSFORM. MEASURE OF SYNCHRONIZATION OF OSCILLATIONS

Studying synchronization of chaotic oscillators various definitions of synchronization have been introduced, namely,
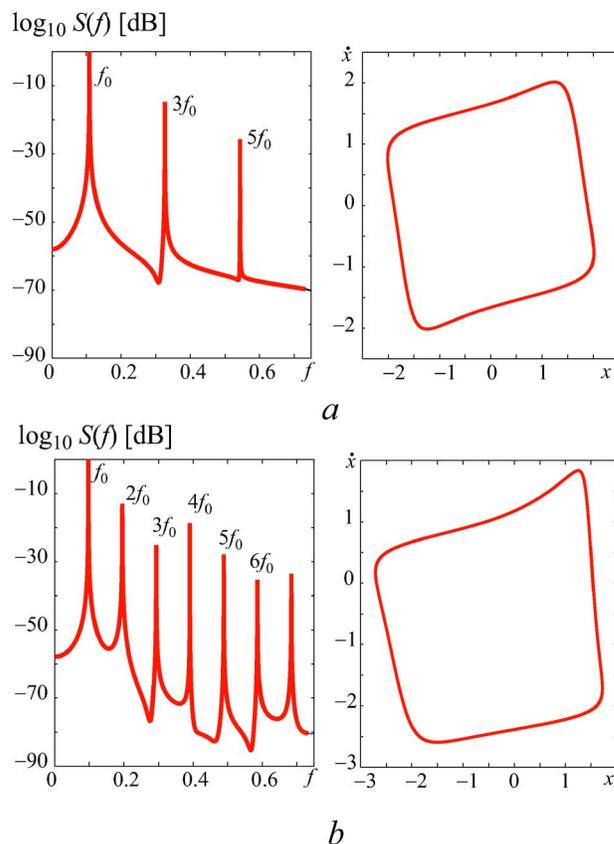

FIG. 1. (Color online) Power spectra and phase portraits for van der Pol oscillator (1) at $K=0$, $\Omega=0.24\pi$, $\mu=1$, and $\alpha=$ (a) 0, (b) 1.

complete synchronization, generalized synchronization, lag synchronization, and phase synchronization [1]. To investigate phase synchronization one has to choose the method of phase definition for the chaotic signals [1,19–21].

We will use the recently proposed approach [22–25] to the analysis of synchronization based on examination of a continuous set of phases defined with the help of the continuous wavelet transform [18,26]

$$W(s,t_0) = \int_{-\infty}^{+\infty} x(t)\psi^*_{s,t_0}(t)dt \qquad (5)$$

of the signal $x(t)$, where $\psi_{s,t_0}(t)$ is the wavelet function related to the mother wavelet $\psi_0(t)$ as

$$\psi_{s,t_0}(t) = \frac{1}{\sqrt{s}}\psi_0\left(\frac{t - t_0}{s}\right). \qquad (6)$$

The time scale s corresponds to the width of the wavelet function $\psi_{s,t_0}(t)$, t_0 is the shift of the wavelet along the time axis, and the asterisk denotes complex conjugation.

We use the Morlet wavelet [27]

$$\psi_0(\eta) = (1/\sqrt[4]{\pi})\exp(j\sigma\eta)\exp(-\eta^2/2) \qquad (7)$$

as the mother-wavelet function. The choice of the wavelet parameter $\sigma=2\pi$ provides the relation $s=1/f$ between the time scale s of the wavelet transform and the frequency f of the Fourier transform.

The wavelet spectrum

$$W(s,t_0) = |W(s,t_0)|\exp[j\phi_s(t_0)] \tag{8}$$

describes the system dynamics for every time scale s at any time moment t_0. The value of $|W(s,t_0)|$ determines the presence and intensity of the time scale s at the moment of time t_0. At the same time, the phase $\phi_s(t) = \arg W(s,t)$ is naturally defined for every time scale s. In other words, it is possible to describe the behavior of every time scale s using its phase $\phi_s(t)$.

If in the signals $x_{1,2}(t)$ there is a range of time scales $s_1 \leq s \leq s_2$ for which the phase locking condition

$$|\Delta\phi_s(t)| = |\phi_{s1}(t) - \phi_{s2}(t)| < \text{const} \tag{9}$$

is satisfied and the part of the wavelet spectrum energy in this range does not vanish,

$$E_{snhr} = \int_{s_1}^{s_2} \langle E(s) \rangle ds > 0, \tag{10}$$

where $\langle E(s) \rangle$ is the distribution of integral energy by time scales defined as $\langle E(s) \rangle = (1/T)\int_t^{t+T}|W(s,t_0)|^2 dt_0$, then the time scales $s \in [s_1;s_2]$ are synchronized and the oscillators are in the regime of time scale synchronization [22]. In Eq. (9) $\phi_{s1,2}(t)$ are the continuous phases of the first and the second oscillator corresponding to the synchronized time scales $s \in [s_1;s_2]$.

Using continuous set of time scales s and the phases associated with these scales we introduce the quantitative measure of chaotic synchronization [22,25]

$$\gamma = \int_{s_1}^{s_2} \langle E(s) \rangle ds \Big/ \int_0^{\infty} \langle E(s) \rangle ds. \tag{11}$$

This measure defines the part of the wavelet spectrum energy falling into the synchronized time scales. The increase of γ from 0 to 1 points to the increase of the part of the wavelet spectrum energy falling into the synchronous time scales s.

IV. INVESTIGATION OF DRIVEN ASYMMETRIC VAN DER POL OSCILLATOR

A. Amplitude dynamics of wavelet spectra of driven oscillator and superimposed signal

Let us consider the wavelet power spectra $|W(s,t)|$ of the external signal $K\sin\varphi(t)$ with linearly varying frequency, the signal $x(t)$ generated by Eq. (1), and the superimposed signal $x_\Sigma(t)$ (4). Typical wavelet power spectra of these signals are presented in Fig. 2.

The analysis of the wavelet power spectrum of the signal a $x(t)$ of a driven van der Pol oscillator [Fig. 2(b)] reveals the classical picture of oscillator frequency locking by the external driving. As a result of this locking, the breaks appear close to the time moments t_s and t_{2s} denoted by arrows, when the driving frequency is close to the frequency of the autonomous oscillator or to its second harmonic. These breaks represent the entrainment of oscillator frequency and its harmonic by external driving. In the region of frequency
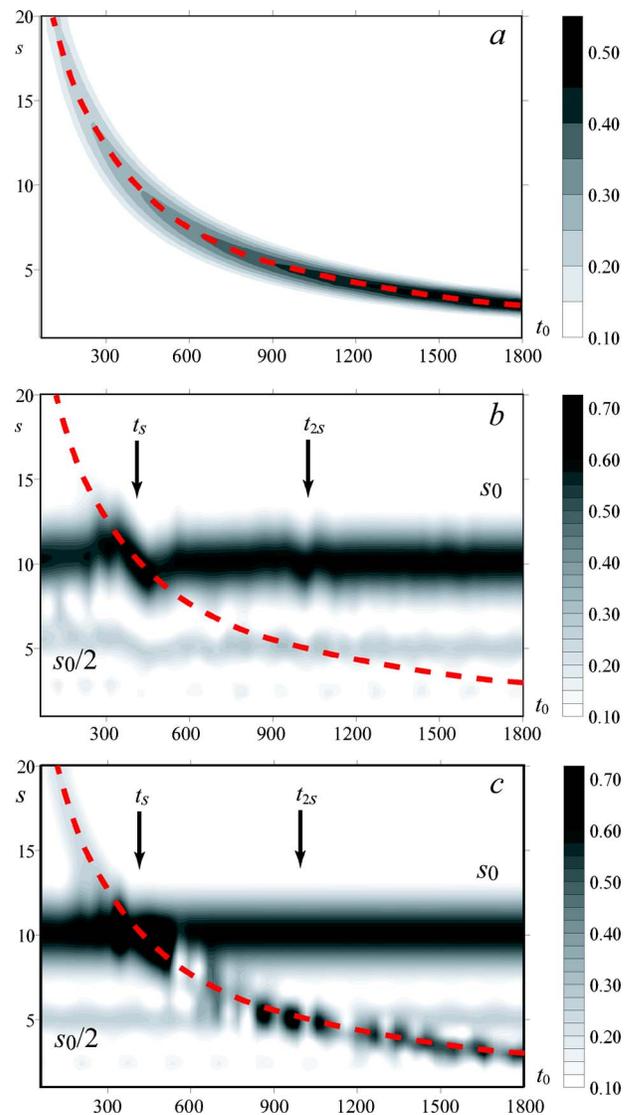

FIG. 2. (Color online) (a) Shaded plot of the wavelet power spectra $|W(s,t_0)|$ for the external signal with the frequency varying in accordance with Eq. (3); (b) the signal generated by oscillator (1); and (c) the superimposed signal (4). Time is shown on the abscissa and time scale is shown on the ordinate. The color intensity is proportional to the absolute value of the wavelet transform coefficients. The scales from the right side of the figure show the values of the coefficients. The dashed lines indicate the time scale $s_d(t)$ corresponding to the linearly increasing frequency $\omega_d(t)$ (3).

entrainment the amplitude of the respective coefficients of the wavelet spectrum increases. This fact agrees well with the known effect of the oscillation amplitude increase in the synchronization (Arnold) tongue. If the detuning $\delta = (\omega_d - 2\pi f_0)$ is great enough, the frequency of oscillations returns to the natural frequency of the autonomous oscillator.

It should be noted that besides the break at the main time scale s_0 of the spectrum, a break at the scale $s_0/2$ corresponding to the second harmonic $2f_0$ takes place. In this region the wavelet surface has no maxima associated with the driving signal since the intensity of the corresponding spectral component is low.

The wavelet power spectrum of the superimposed signal $x_\Sigma(t)$ is shown in Fig. 2(c). In contrast to the previous case, the dynamics of both the van der Pol oscillator and the external force with varying frequency are well pronounced in the spectrum. The absence of a break in the neighborhood of the time moment t_s indicates the absence of entrainment of the oscillator frequency. One can see only slight distortion of the wavelet surface caused by the increase of the wavelet coefficients amplitude $|W|$ at time moments close to t_s. This effect is the result of the addition of two signals with comparable amplitudes and close frequencies. Furthermore, the surface distortion in the region of the main scale s_0 is not followed by any change in the wavelet spectrum at the scale $s_0/2$ corresponding to the second harmonic of the signal $x(t)$. Similarly, the coincidence of the frequencies ω_d and $4\pi f_0$ at the time moment t_{2s} is not followed by any changes of the dynamics at the main scale s_0.

Thus, it is possible to distinguish the cases of synchronization and mixing of the signals by analyzing the dynamics of time scales corresponding to the basic frequency and its harmonics in the wavelet power spectrum. In the case of mixing the changes in the dynamics of the scale having a frequency that is close to the driving frequency do not lead to any change in the dynamics of other time scales. In the case of synchronization the typical break in the wavelet power spectrum is observed at all characteristic time scales.

B. Phase dynamics of driven oscillator and superimposed signal

Let us consider the phase difference between the $x(t)$ signal produced by Eq. (1) and the external signal with linearly increasing frequency and the phase difference between the $x_\Sigma(t)$ signal produced by Eq. (4) and the external signal. The phase differences $\Delta\phi_s(t)$ are calculated along the scale $s_d(t)$, corresponding to the linearly increasing frequency (3), i.e., along the dashed lines in Fig. 2. Typical dependencies $\Delta\phi_s(t)$ are presented in Fig. 3.

First, we consider the case of linear mixing of the signals and analyze the phase dynamics in the vicinity of $t=t_s$, where the driving frequency is close to the basic frequency of the van der Pol oscillator: $\omega_d(t_s) \approx 2\pi f_0$. The phase dynamics at the main scale $s_0 = 1/f_0$ of the van der Pol oscillator can be written as $\phi_{s0}(t) = 2\pi f_0 t + \varphi_0$, where φ_0 is the initial phase. The phase $\phi_s(t)$ of the driving signal is determined by Eq. (2). Under the assumption that the amplitude of the external signal is significantly smaller than the amplitude of oscillations of the van der Pol oscillator, the temporal behavior of the phase difference between the components of the superimposed signal $x_\Sigma(t)$ takes the form

$$\Delta\phi_s(t) = \phi_{s0}(t) - \phi_s(t) = 2\pi[(f_0 - a)t - (b/T)t^2] + \varphi_0. \tag{12}$$

It follows from Eq. (12) that the phase difference varies under a parabolic law and the parabola has an extremum at $t=t_s$. In the neighborhood of this moment of time the dependence $\Delta\phi_s(t)$ is symmetric with respect to $t=t_s$. A similar situation takes place at the scale $s_0/2 = 1/(2f_0)$ corresponding to the second harmonic.
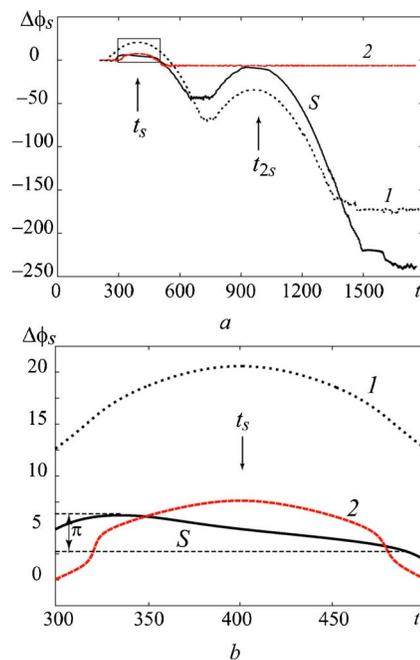

FIG. 3. (Color online) Phase differences between the superimposed signal (4) and the external signal with linearly increasing frequency (curves 1 and 2) and between the signal of the driven van der Pol oscillator (1) and the driving signal (curve S). $R=0.2$ for the curve 1 and 1.0 for the curve 2, and $K=0.2$ for the curve S. The phase differences are calculated at the scale $s_d = 2\pi/\omega_d$. The fragment marked in (a) is enlarged in (b).

Such behavior of $\Delta\phi_s(t)$ is illustrated by curves 1 and 2 in Fig. 3. The curve 1 is plotted for small amplitude of the external force and has a parabolic shape in the neighborhood of t_s and t_{2s}. The curve 2 plotted for a greater amplitude R also has an extremum at $t=t_s$. However, this extremum is less pronounced and has a shape different from a quadratic one. This is explained by a great influence of the external signal having amplitude comparable with the amplitude of the signal generated by the van der Pol oscillator. This case is characterized by an almost constant phase difference which is close to zero at t far from t_s. For large R values the part of the external signal in the mixture $x_\Sigma(t)$ is sufficiently large. As a result, a phase difference is calculated between the phases of practically the same signals. Therefore, if the part of the driving signal is large enough in the superimposed signal, one can detect spurious synchronization using conventional methods of synchronization investigation.

Let us consider now the case of synchronization of an asymmetric van der Pol oscillator by external driving with linearly increasing frequency. This case is illustrated by the curve S in Fig. 3.

We analyze the behavior of the phase difference $\Delta\phi_s(t)$ using the method of slowly varying amplitudes under the assumption that the external driving does not change significantly the amplitude of nonautonomous oscillations but mainly has an influence on the phase relationships. It can be shown that $\Delta\phi_s(t)$ is governed by the Adler equation [28]
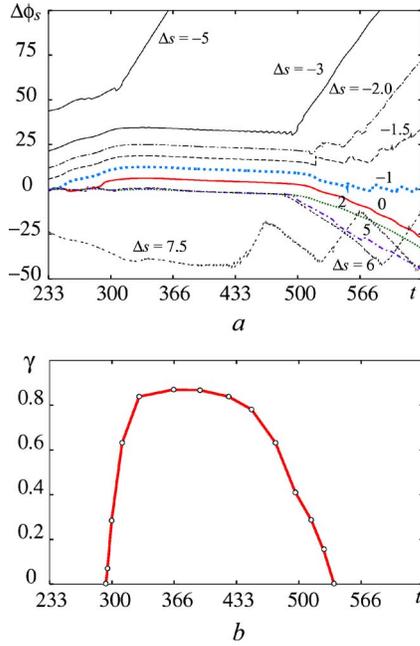
FIG. 4. (Color online) (a) Phase differences $\Delta\phi_s(t)$ between the driven asymmetric van der Pol oscillator and the driving signal at scales $s_d(t)+\Delta s$. (b) Measure of synchronization γ.

$$\frac{d[\Delta\phi_s(t)]}{dt} + \kappa \sin \Delta\phi_s(t) - [2\pi f_0 - \omega_d(t)] = 0, \quad (13)$$

where κ is the coefficient defined by the oscillator parameters. It follows from the Adler equation that in the region of synchronization defined by the condition $[2\pi f_0 - \omega_d(t)] \leqslant \kappa$ the phase difference $\Delta\phi_s(t)$ monotonically decreases by π under driving frequency variation. By this is meant that in the case of the synchronization of the oscillator by external driving with linearly varying frequency we will observe in the vicinity of time moments t_s and t_{2s} the regions where the phase difference varies over π. This situation is illustrated by the curve S in Fig. 3.

A special feature of our approach for detecting synchronization is the application of external driving with varying frequency. Another important feature of our method is the analysis of the phase difference between the signals at different time scales s [22,29]. We consider the behavior of the phase difference $\Delta\phi_s(t)$ at the scales $s(t)=s_d(t)+\Delta s$, where Δs is the detuning of the scale with respect to the basic scale $s_d(t)$.

In Fig. 4(a) the phase differences at various scales are presented for the case when ω_0 is close to ω_d. It can be seen from the figure that for $\Delta s \in (-1,2)$ the phase dynamics is qualitatively similar to the case of accurate adjustment to the basic scale $s_d(t)$. At greater Δs values the duration of epochs of synchronous behavior becomes shorter and beginning from some values of detuning there is no synchronization at all. The presence of a range of scales Δs within which synchronous dynamics is observed allows one to investigate the system behavior without accurate adjustment of the scale to the basic scale $s_d(t)$ varying in time. It can be useful for the analysis of experimental data.
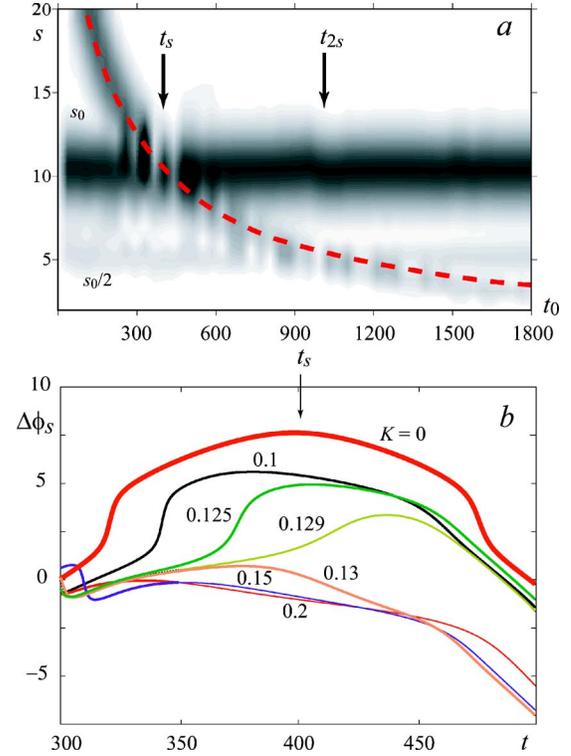

FIG. 5. (Color online) (a) Wavelet power spectrum $|W(s,t_0)|$ for the superposition of the signal of driven oscillator (1) with $K=0.125$ and the external forcing with $R=1$. (b) Phase difference at the scale $s_d(t)$ between the external forcing with $R=1$ and the superposition of the external forcing and the driven oscillator (1) signal with different K values.

Figure 4(b) illustrates the dependence of the measure of synchronization γ defined by Eq. (11) on time. At $t \gtrsim 300$ the system quickly comes to the regime of time scale synchronization. The part of the wavelet spectrum energy falling into the synchronized time scales is more than 80%. With further increase of time the value of γ decreases and at $t>540$ it becomes equal to zero. The last case corresponds to the absence of synchronization.

C. Dynamics of nonautonomous system in the simultaneous presence of mixing and synchronization

Let us consider now the situation when the effects of mixing and synchronization of the signals of the self-sustained oscillator and external driving are simultaneously present. Figure 5(a) shows the amplitude spectrum $|W(s,t_0)|$ of the wavelet transform for the signal being the superposition of the driven oscillator (1) signal synchronized by external driving with the amplitude $K=0.125$ and the driving signal itself with $R=1$. This spectrum has features inherent to both the cases of synchronization and mixing and gives no definite answer to the question about the nature of the underlying dynamics. The analysis of phase dynamics appears to be more informative.

Figure 5(b) shows the dynamics of phase differences $\Delta\phi_s(t)$ for $R=1$ and various amplitudes K. At small K values the situation is qualitatively similar to the case of mixing

without synchronization considered above. The regime of synchronization appears in a certain range of frequencies as the amplitude K increases. The variation of the phase difference in the synchronization tongue takes the form of an inclined line. The boundaries of this line correspond to the loss of synchronization. Note that the variation of the phase difference in the synchronization region in Fig. 5(b) is smaller than in the case of $R=0$.

V. INVESTIGATION OF SYNCHRONIZATION BETWEEN THE RESPIRATION AND THE PROCESS OF BLOOD PRESSURE SLOW REGULATION

This section contains the results of physiological data analysis. We studied eight healthy young male subjects having average levels of physical activity. The signals of ECG and respiration were simultaneously recorded in the sitting position with the sampling frequency 250 Hz and 16-bit resolution. The experiments were carried out under paced respiration with the breathing frequency linearly increasing from 0.05 to 0.3 Hz. The rate of breathing was set by sound pulses. The duration of experiments was 30 min.

Figure 6(a) shows a typical respiratory signal with linearly increasing frequency and its wavelet power spectrum [Fig. 6(b)]. Extracting from the ECG signals the sequence of R-R intervals, i.e., the series of the time intervals between the two successive R peaks, we obtain information about the heart rate variability. A typical sequence of R-R intervals for breathing at linearly increasing frequency is shown in Fig. 6(c). Since the sequence of R-R intervals is not equidistant, we developed a technique for applying the continuous wavelet transform to nonequidistant data. Figure 6(d) shows the wavelet spectrum $|W(s,t_0)|$ for the sequence of R-R intervals presented in Fig. 6(c). This wavelet spectrum demonstrates the high-amplitude component denoted as 1 corresponding to the varying respiratory frequency manifesting itself in the HRV data. The second harmonic of the respiration is observed at a twice higher frequency. The power of the rhythm with the basic frequency of about 0.1 Hz is rather small and this frequency is not pronounced in the spectrum. The amplitude of the respiratory rhythm in R-R intervals is much higher than the amplitude of the rhythm with the frequency 0.1 Hz. Comparing the wavelet spectrum of R-R intervals under linearly increasing frequency of respiration with the wavelet spectra presented in Secs. III and IV one can come to the conclusion that a significant mixing of the considered physiological signals takes place without synchronization. However, the investigations performed in Ref. [11] with the same experimental data have clearly shown the presence of 1:1 synchronization between the process of blood pressure slow regulation and respiration at breathing frequencies close to 0.1 Hz. This synchronization has been observed within the time interval 200–600 s for each of the subject studied. The wavelet spectrum in Fig. 6(d) does not allow us to detect the presence of synchronization. The increase of HRV amplitude at frequencies close to 0.1 Hz can be regarded only as an indirect indication of the presence of synchronization.

In Fig. 7(a) the phase difference between the R-R intervals and respiration is presented. Between 200 and 600 s the
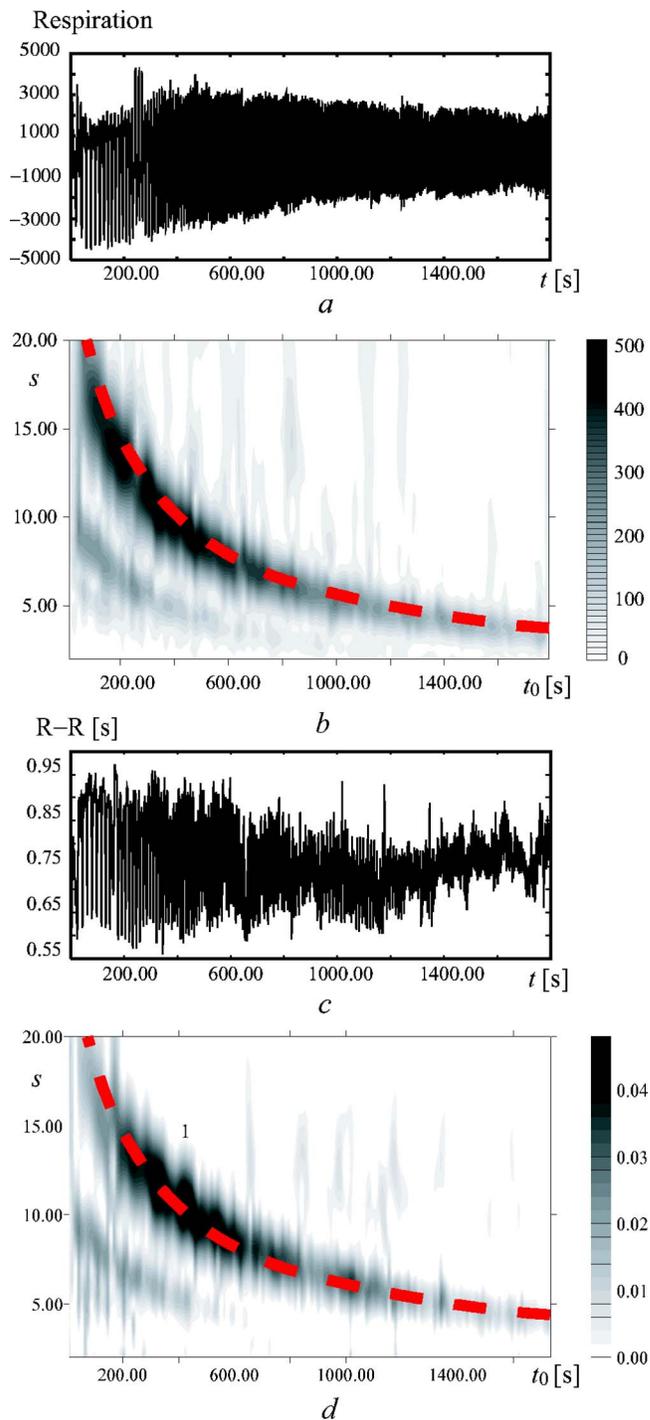

FIG. 6. (Color online) Typical time series of breathing with linearly increasing frequency (a) and its wavelet power spectrum (b). The respiratory signal is in arbitrary units. Sequence of R-R intervals for the case of respiration with linearly increasing frequency (c) and its wavelet power spectrum (d). The dashed lines indicate the time scale corresponding to linearly increasing frequency of respiration.

phase varies on average almost linearly at the scale $s = s_b(t) = 1/f_b(t)$, where f_b is the linearly increasing frequency of breathing. In this time interval the phase variation is close to π indicating the presence of synchronization. Outside of the
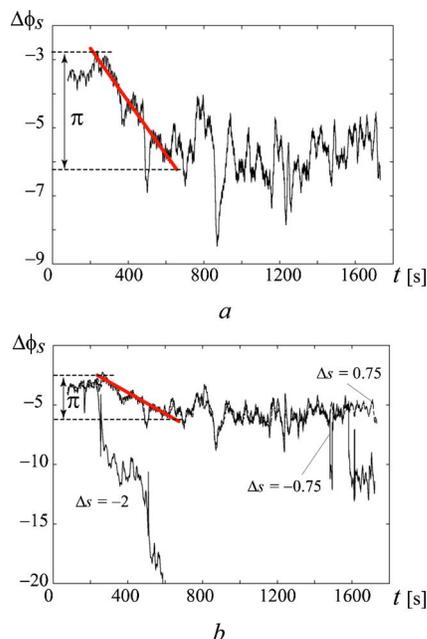
FIG. 7. (Color online) Phase differences between R-R intervals and respiratory signal with linearly increasing frequency. The phase differences are calculated at the linearly varying scale $s_b(t) = 1/f_b(t)$ (a) and scales $s_b(t) + \Delta s$ (b).

synchronization region the phase difference fluctuates around a constant value. From the result obtained it may be concluded that the respiratory dynamics manifested in the R-R intervals affects the rhythm of blood pressure regulation within the time interval 200–600 s. Outside of this interval the respiratory component is observed in R-R intervals as a result of mixing of the signals without their interaction.

A similar behavior of the phase difference is observed at neighboring time scales. Figure 7(b) shows phase differences at the scales $s = s_b(t) + \Delta s$. For small detuning ($\Delta s = \pm 0.75$) the phase dynamics is qualitatively similar to the dynamics at the scale $s = s_b$. Hence, a small error in determining the required scale will not result in qualitative changes in the plot. If the mismatch of the scale of observation and the scale of respiration s_b is large, the amplitude of the corresponding rhythm decreases and its phase cannot be defined confidently. This is the case $\Delta s = -2$ in Fig. 7(b). As a result, the phase difference is no longer constant.

VI. CONCLUSION

We have shown that applying external driving with varying frequency to the self-sustained oscillator and using a method based on wavelet transform one can distinguish the case of synchronization of an oscillator by this driving signal from the case of absence of synchronization. The method allows one to detect the presence of synchronization between signals with close frequencies even in the case when the effect of mixing of the signals is present. The use of a driving signal with varying frequency is crucial for the proposed method, since calculation of the phase difference between the superimposed signals at a fixed time scale gives no answer to the question of whether the system response is the result of active interaction of the oscillating processes or the result of their mixing without changes of the underlying dynamics. The proposed method does not require accurate adjustment of the scale of observation to the time scale associated with the varying frequency of the external driving. The efficiency of the continuous wavelet transform for estimation of the signal phase is demonstrated with experimental physiological data characterized by high level of noise.

The proposed technique is applicable to a situation with superimposed signals being at our disposal, and it is necessary to define whether system 1 with adjustable frequency affects system 2 and can synchronize it. Such information can be useful, for example, for the diagnostics of the cardiovascular system state. Synchronization between the rhythmic processes in the human cardiovascular system under paced respiration is less effective in patients than in healthy subjects, and this effect correlates with the seriousness of the heart failure [30]. Using a small variation of the relative phase or high values of the phase synchronization index as criteria of synchronization, one can come to wrong biological conclusions due to the mixing of the analyzed signals.

The proposed method can be used for detecting synchronization in different systems if it is possible to vary the frequency of the external driving in the experiment.

[1] A. Pikovsky, M. Rosenblum, and J. Kurths, *Synhronization: A Universal Concept in Nonlinear Sciences* (Cambridge University Press, Cambridge, U.K., 2001).

[2] L. Glass and M. C. Mackey, *From Clocks to Chaos: The Rhythms of Life* (Princeton University Press, Princeton, NJ, 1988).

[3] L. Glass, Nature (London) **410**, 277 (2001).

[4] E. Mosekilde, Yu. Maistrenko, and D. Postnov, *Chaotic Synchronization: Applications to Living Systems*, Ser. A (World Scientific, Singapore, 2002), Vol. 42.

[5] C. Schäfer, M. G. Rosenblum, H. -H. Abel, and J. Kurths, Phys. Rev. E **60**, 857 (1999).

[6] S. Boccaletti, J. Kurths, G. Osipov, D. L. Valladares, and C. Zhou, Phys. Rep. **366**, 1 (2002).

[7] F. C. Meinecke, A. Ziehe, J. Kurths, and K. -R. Müeller, Phys. Rev. Lett. **94**, 084102 (2005).

[8] A. Stefanovska and M. Hočič, Prog. Theor. Phys. Suppl. **139**, 270 (2000).

[9] M. Bračič-Lotrič and A. Stefanovska, Physica A **283**, 451 (2000).

[10] N. B. Janson, A. G. Balanov, V. S. Anishchenko, and P. V. E. McClintock, Phys. Rev. E **65**, 036212 (2002).

[11] M. D. Prokhorov, V. I. Ponomarenko, V. I. Gridnev, M. B. Bodrov, and A. B. Bespyatov, Phys. Rev. E **68**, 041913 (2003).

[12] S. Rzeczinski, N. B. Janson, A. G. Balanov, and P. V. E. McClintock, Phys. Rev. E **66**, 051909 (2002).

[13] N. B. Janson, A. G. Balanov, V. S. Anishchenko, and P. V. E. McClintock, Phys. Rev. E **65**, 036211 (2002).

[14] A. G. Rossberg, K. Bartholomé, H. U. Voss, and J. Timmer, Phys. Rev. Lett. **93**, 154103 (2004).

[15] J. Jamšek, A. Stefanovska, P. V. E. McClintock, and I. A. Khovanov, Phys. Rev. E **68**, 016201 (2003).

[16] J. Jamšek, A. Stefanovska, and P. V. E. McClintock, Phys. Med. Biol. **49**, 4407 (2004).

[17] V. I. Ponomarenko, M. D. Prokhorov, A. B. Bespyatov, M. B. Bodrov, and V. I. Gridnev, Chaos, Solitons Fractals **23**, 1429

(2005).

[18] M. G. Rosenblum, A. S. Pikovsky, and J. Kurths, Phys. Rev. Lett. **76**, 1804 (1996).

[19] A. Pikovsky, M. Rosenblum, and J. Kurths, Int. J. Bifurcation Chaos Appl. Sci. Eng. **10**, 2291 (2000).

[20] V. S. Anishchenko and T. E. Vadivasova, J. Commun. Technol. Electron. **47**, 117 (2002).

[21] A. E. Hramov and A. A. Koronovskii, Chaos **14**, 603 (2004).

[22] A. E. Hramov, A. A. Koronovskii, M. K. Kurovskaya, and O. I. Moskalenko, Phys. Rev. E **71**, 056204 (2005).

[23] A. E. Hramov and A. A. Koronovskii, Physica D **206**, 252 (2005).

[24] A. E. Hramov and A. A. Koronovskii, JETP Lett. **79**, 316 (2004).

[25] A. A. Koronovskii and A. E. Hramov, *Continuous Wavelet Analysis and Its Applications* (Fizmatlit, Moscow, 2003).

[26] *Wavelets in Physics*, edited by J. C. Van den Berg (Cambridge University Press, Cambridge, U.K., 2004).

[27] A. Grossman and J. Morlet, SIAM J. Math. Anal. **15**, 273 (1984).

[28] R. Adler, Proc. IRE **34**, 351 (1949).

[29] A. E. Hramov, A. A. Koronovskii, P. V. Popov, and I. S. Rempen, Chaos **15**, 013705 (2005).

[30] N. Ancona, R. Maestri, D. Marinazzo, L. Nitti, M. Pellicoro, G. D. Pinna, and S. Stramaglia, Physiol. Meas **26**, 363 (2005).